PROCEEDINGS OF SCIENCE

Lepton Flavour Universality measurements and flavour anomalies at LHCb

Guillaume Pietrzyk

IJCLab, CNRS, Université Paris-Saclay
Orsay, France

E-mail: guillaume.pietrzyk@cern.ch

This document presents two new results of the LHCb experiment investigating B flavour anomalies. The first result provides a new measurement of the branching fraction ratios $R(D^+)$ and $R(D^{*+})$ using muonic τ decays as a test of lepton flavour universality. The second result offers a comprehensive analysis of local and nonlocal amplitudes in the rare $B^0 \to K^{*0}\mu^+\mu^-$ decay, disentangling potential New Physics contributions from Standard Model nonlocal effects. Both analyses yield results compatible with previous measurements, with the tension between theory and experiment in $R(D^{(*)})$ reaching a significance of 3.2σ. Furthermore, a 2.1σ deviation in the Wilson coefficient C_9 is observed in the $B^0 \to K^{*0}\mu^+\mu^-$ decay. These measurements contribute to the growing body of evidence hinting at possible New Physics contributions in B meson decays.

12th Large Hadron Collider Physics Conference (LHCP2024)
3-7 June 2024
Boston, USA

PoS(LHCP2024)079

1. Introduction

The predictions of the Standard Model (SM) of particle physics, describing the properties and interactions of elementary particles, have been experimentally confirmed since the introduction of the model more than fifty years ago. However, the SM cannot describe experimental data such as the dark-matter content or the large dominance of matter over antimatter in the observable universe. The particle physics community has therefore been looking for experimental signatures of *New Physics* (NP), that could account for the experimental data. The first approach, described by the *high energy frontier*, consists in increasing the energy of particle colliders to produce directly NP particles. The second approach, being the subject of this document, is described by the *high intensity frontier* and investigates deviations between SM theoretical predictions and experimental data at high level of statistical precision. These deviations can be made possible through the presence of virtual NP particles in quantum processes accessible at the centre-of-mass energies of current particle physics experiments.

In recent years, the LHCb experiment [1, 2], one of the four experiments of the Large Hadron Collider (LHC), has observed such experimental deviations in the decays of B mesons, known as the *B flavour anomalies* [3–10]. These proceedings present two recent results, giving new insights on the current status of the flavour anomalies. The first result constitutes a new measurement of the branching fraction ratios $R(D^+)$ and $R(D^{*+})$ using muonic τ decays [11], while the second result consists of a comprehensive analysis of local and nonlocal amplitudes in the $B^0 \to K^{*0}\mu^+\mu^-$ decays [12].

2. Measurement of the branching fraction ratios $R(D^+)$ and $R(D^{*+})$ using muonic τ decays

Semileptonic b-hadron decays involving a $b \to c$ quark transition proceed in the SM at the tree level through the exchange of a virtual W boson. An accidental symmetry of the SM, known as *lepton flavour universality* (LFU) implies that the three SM leptons, electron (e^-), muon (μ^-) and tau (τ), have the same interaction strengths, apart from the different lepton masses. LFU can be tested through the ratios of branching fractions $R(D^{*+})$ and $R(D^+)$, defined coherently as

$$R\left(D^{(*)+}\right) \equiv \frac{\mathcal{B}\left(\bar{B}^0 \to D^{(*)+}\tau^-\bar{\nu}_\tau\right)}{\mathcal{B}\left(\bar{B}^0 \to D^{(*)+}\mu^-\bar{\nu}_\mu\right)}\,. \tag{1}$$

A statistically significant departure of $R(D^{(*)+})$ from the SM prediction is interpreted as a clear signature of physics beyond the SM (BSM). Recently, the LHCb collaboration measured $R(D^{(*)+})$ with leptonic τ decays [9] and $R(D^{*+})$ with hadronic τ decays [10]. The current combined world average value of $R(D^{(*)+})$ yields a 3.3σ tension with the SM expectation [3].

The new result presented in this document corresponds to the first $R\left(D^{(*)+}\right)$ measurement with D^+-meson decays [11]. The analysis uses proton–proton (pp) collision data collected by the LHCb detector in 2015 and 2016, corresponding to an integrated luminosity of $2\,\text{fb}^{-1}$. The measurement exploits the $D^{*+} \to D^+(\to K^-\pi^+\pi^+)\pi^0$ channel, with unreconstructed π^0 decays. In addition, the τ decays via the $\mu\bar{\nu}_\mu\nu_\tau$ channel with undetected neutrinos. As a result, all four studied decays of this analysis (shown in Eq. (1)) have a common $K^-\pi^+\pi^+\mu^-$ final state, allowing for a

simultaneous measurement of $R\left(D^{(*)+}\right)$ with the same dataset. In this analysis, the tauonic decays are referred to as the signal channel while the muonic decays are denoted as the normalisation channel. Experimentally, Eq. (1) can be expressed as

$$R\left(D^{(*)+}\right) = \frac{\varepsilon_{\mu}^{D^{(*)+}}}{\varepsilon_{\tau}^{D^{(*)+}}} \frac{N_{\tau}^{D^{(*)+}}}{N_{\mu}^{D^{(*)+}}} \frac{1}{\mathcal{B}\left(\tau^- \to \mu^- \bar{\nu}_{\tau} \nu_{\mu}\right)} \tag{2}$$

where ε describes the efficiency obtained from simulation and N represents the signal and normalisation yields. These yields are obtained via a three-dimensional likelihood fit to the squared four-momentum transferred to the lepton system q^2, the invariant-mass of unreconstructed particles m^2_{miss} and the lepton energy in the $\bar{B}^0$ rest frame E^*_l.

An online signal candidate selection is performed by a trigger system that consists of a hardware stage, based on information from the calorimeter and muon chamber detectors, followed by a software stage, that distinguishes tauonic from muonic decays [13]. The D^+-meson production vertex is required to be significantly displaced from the pp collision point, while its four children candidates are subjected to kinematic, topological and particle identifications criteria. In addition, Boosted Decision Tree (BDT) algorithms are employed to suppress background originating from fake, combinatorial and partially reconstructed candidates. The residual fake-D^+ background is subtracted using the *sPlot* technique from a fit to the $K^-\pi^+\pi^+$ invariant mass [14]. A BDT-based isolation tool is used to classify tracks based on their consistency with the signal B-decay vertex. The data sample is then split into four distinct regions based on the BDT response. The first, the *signal region*, requires that no track is close to the signal candidate. Two other regions, the 1π and 2π *regions*, include partially reconstructed decays such as $B \to D^*_0(2300)(\to D\pi)\mu\nu_{\mu}$ or $B \to D^*(2640)^{\pm}(\to D^*(2010)^+\pi^+\pi^-)\mu\nu_{\mu}$. Finally, the $1K$ *region* includes background contributions from $\bar{B} \to D^+(X_c \to \mu^- X)(X')$, where X_c is a charm hadron and X represents any number of particles that are not reconstructed.

Simulation samples are employed to compute efficiencies and determine probability density functions (PDF). Computing time is significantly reduced by using *Tracker-Only* simulation, where the response from the RICH, calorimeter and muon detectors is turned off. Model disagreements between data and simulation are treated through a reweighting of particle kinematics, and a description of $D^+ \to K^-\pi^+\pi^+$ Dalitz resonances and soft-photon corrections [15]. The PDFs of signal, normalisation and background components are parametrised as histogram templates. The signal and $B \to D^{**}X$-like background form factors [16–18] are allowed to vary in the fit using the HAMMER software tool implemented in RooFit [19–21]. The combinatorial background is modelled using reconstructed same-sign $D^+\mu^+$ candidates, while muon mis-identification templates are obtained from dedicated experimental control samples.

Figure 1 presents the three fit variables q^2, m^2_{miss} and E^*_{μ} in the signal region, with the fit results overlaid. Both signal and normalisation channels are displayed in dark blue and blue, respectively. The LFU observables are determined to be

$$R(D^+) = 0.249 \pm 0.043 \pm 0.047\,, \qquad R(D^{*+}) = 0.402 \pm 0.081 \pm 0.085\,, \tag{3}$$

where the first uncertainties are statistical and the second systematic. The correlation factor between both measured is measured to be $\rho = -0.39$. The main sources of systematic uncertainties are related to background modelling and form-factor parametrisations.

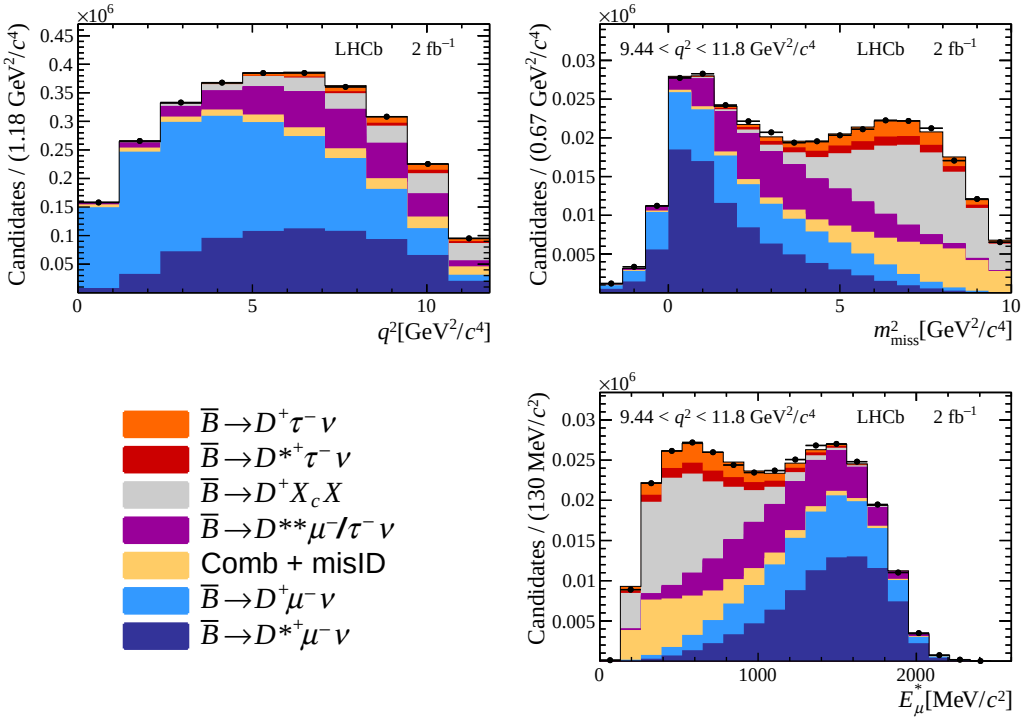

Figure 1: Distributions of the three kinematic variables in the signal isolation region, with the fit result overlaid. The q^2 distribution is shown over the full fit range while $m^2_{\rm miss}$ and E^*_μ are only shown in the range $9.44 < q^2 < 11.8\,\text{GeV}^2/c^4$.

The new results presented in this document are included in an updated HFLAV average [3], shown in Fig. 2, and are seen to be compatible with both the world average value (red contour) and the SM expectation (black point). The tension between experimental world average and theory is measured to be at the 3.2σ significance level.

3. Comprehensive analysis of local and nonlocal amplitudes in the $B^0 \to K^{*0}\mu^+\mu^-$ decays

In recent years, the $B^0 \to K^{*0}\mu^+\mu^-$ decay has attracted active interest from the particle physics community. Indeed, its differential decay rate and various of its angular observables have indicated tensions with the SM expectations [4–8]. The decay proceeds through a $b \to s\mu\mu$ loop suppressed flavour-changing neutral current, and profits from the rich information of the multitude of K^{*0} polarisation amplitudes. These aspects make the $B^0 \to K^{*0}\mu^+\mu^-$ decay an ideal candidate to look for BSM contributions. The $b \to s\mu\mu$ transition can be described by an effective field theory (EFT) [24], with the Wilson Coefficients (WCs) $C_7^{(\prime)}$, $C_9^{(\prime)}$ and $C_{10}^{(\prime)}$ describing the left-handed (right-handed) electromagnetic, vector and axial-vector short-distance contributions, respectively. The effective WCs have components related to both local and nonlocal contributions. The local contributions are related to energy scales well above the B-meson masses where NP effects can manifest themselves. On the contrary, leading nonlocal contributions are due to narrow

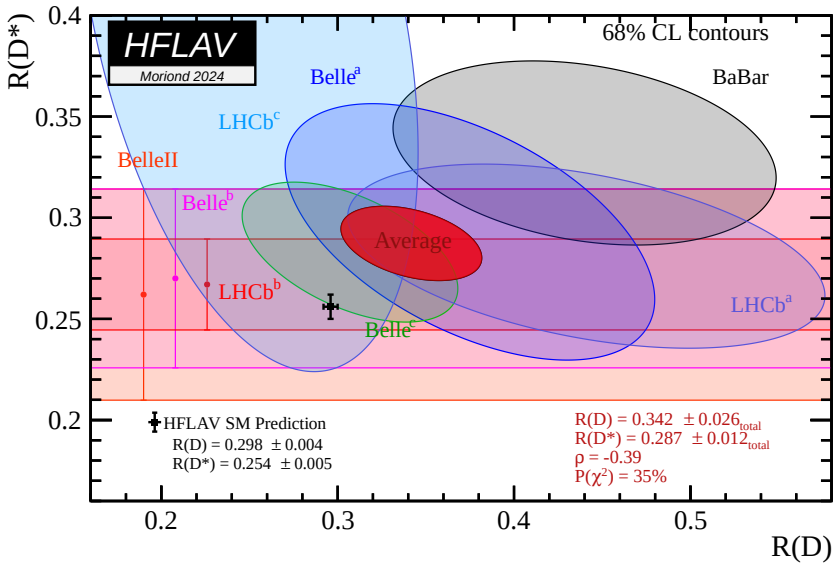

Figure 2: Measurements of $R(D)$ and $R(D^*)$ and their two-dimensional averages, where contours correspond to a 68% confidence level (CL). The results presented in this document are shown in light blue under LHCb^c. The theoretical predictions [22, 23], in black, and the experimental average, in red, deviate by a 3.2σ significance.

charmonium resonances, which are often vector-like and can significantly impact the measured value of C_9, mimicking BSM effects.

The measurement described is the first to model both one-particle and two-particle nonlocal amplitudes, allowing to disentangle explicitly local from nonlocal contributions [12]. This measurement analyses for the first time the full $B^0 \to K^{*0}\mu^+\mu^-$ Run 1 (2011–2012) and Run 2 (2016–2018) LHCb dataset, corresponding to an integrated luminosity of $8.4\,\text{fb}^{-1}$. The analysis performs an unbinned measurement of angular distributions through a parametrization of the full dimuon invariant mass q^2 ($q^2 \in [0.1, 18.0]\,\text{GeV}^2/c^4$) and the three decay angles $\Omega \equiv (\cos\theta_K, \cos\theta_l, \phi)$. The experimental data sample is used to model background contributions and determine $K^{*0}(892)$ S-wave parameters. Simulation samples are employed to model selection, reconstruction, detection and resolution effects through the determination of an acceptance function. External theoretical inputs are used to describe local form factors that are Gaussian-constrained in the fit. The final fit to data extracts 150 parameters, that include WCs and nonlocal model parameters.

The measured effective C_9 WC can be separated according to local and nonlocal contributions in the following way:

$$C_9^{\text{eff},\lambda}(q^2) = C_9^{\mu} + Y_{c\bar{c}}^{(0),\lambda} + Y_{c\bar{c}+\text{light}}^{1\text{P},\lambda}(q^2) + Y_{c\bar{c}}^{2\text{P},\lambda}(q^2) + Y_{\tau\bar{\tau}}(q^2)\,, \tag{4}$$

where λ refers to the helicity dependence, while the Y elements are q^2-dependent nonlocal terms related to one- and two-particle contributions. The term $Y_{c\bar{c}}^{(0),\lambda}$ is a subtraction term whose value is estimated from calculations at negative q^2 values [25]. The model allows for the inclusion of the $Y_{\tau\bar{\tau}}(q^2)$ term, allowing for the first direct measurement of $C_{9\tau}$ from $B^0 \to K^{*0}\tau^+\tau^-$ decays,

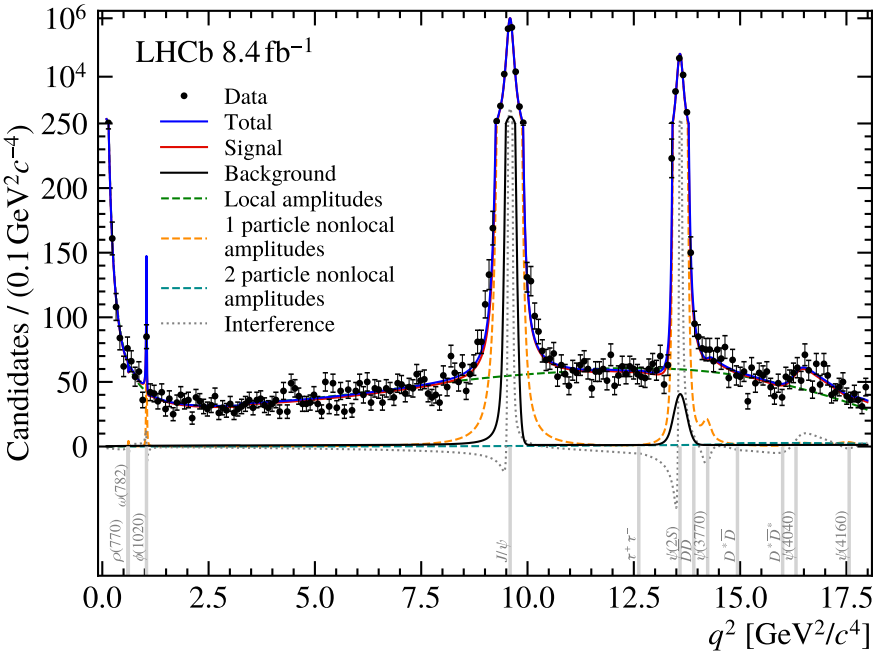

Figure 3: Fit to the q^2 distribution in the data sample. The total PDF, in blue, is decomposed into signal and background components. The signal is further decomposed into local and nonlocal contributions, as described in Eq.(4). The y-axis includes a logarithmic scale at high values to incorporate the imposing J/ψ and $\psi(2S)$ peaks.

exploiting the rescattering of τ leptons into a muon pair. Finally, the term C_9^μ describes local penguin contributions and are directly compared to SM expectations.

The final fit to data, shown in Fig. 3, allows for a complete and precise description of the q^2 spectrum. The local WCs are measured to be

$$\begin{aligned} C_9 &= 3.56 \pm 0.28 \pm 0.18\,, \\ C_{10} &= -4.02 \pm 0.18 \pm 0.16\,, \\ C_9' &= 0.28 \pm 0.41 \pm 0.12\,, \\ C_{10}' &= -0.09 \pm 0.21 \pm 0.06\,, \\ C_{9\tau} &= (-1.0 \pm 2.6 \pm 1.0) \times 10^2\,, \end{aligned}$$

where the first uncertainties are statistical and the second systematic. The largest deviation from the SM expectation is seen via $\Delta C_9^{\rm NP} = C_9 - C_9^{\rm SM} = -0.71 \pm 0.33$, corresponding to a 2.1σ deviation. The complete set of results is in agreement with previous analyses from the LHCb experiment. The global significance of the analysis results is measured to be at the 1.5σ level.

Figure 4 presents the experimental results of the angular observable P_5'. Figure 4a displays the observable with and without nonlocal contributions, where it becomes apparent that nonlocal effects influence the observables values. Figure 4b compares the SM prediction of P_5' (yellow) to their experimental determination, with (cyan) and without (red) setting the values of the WCs to their SM values. The difference between the cyan and red bands show that NP contributions can

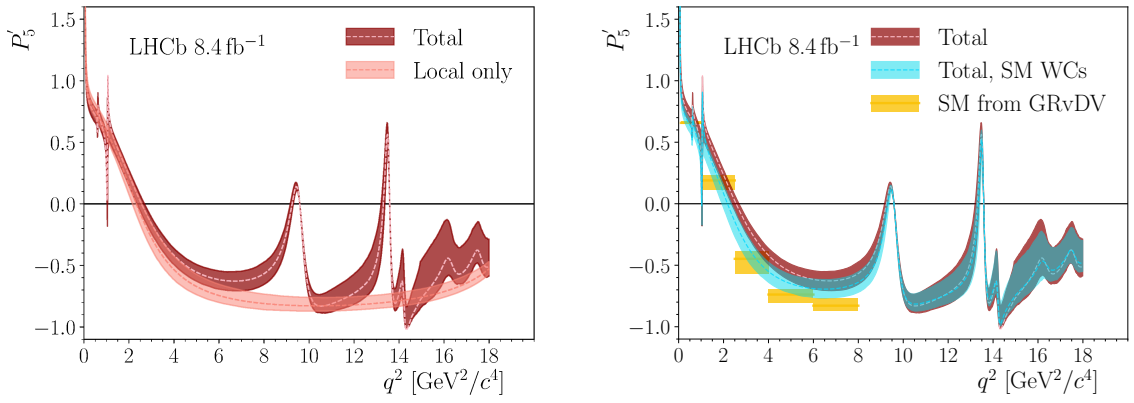

(a) **(b)**

Figure 4: Distribution of the angular observable P_5' extracted from a fit to the data. In (a) P_5' is shown with and without the nonlocal contributions. In (b) the total distribution is compared to the SM expectation setting or not the WCs to their SM expectations. For both subfigures the shaded bands correspond to 68% confidence regions.

have non-negligible impact on the experimental values. Additionally, the cyan experimental band and the SM expectations differ, indicating that the current theoretical predictions may underestimate nonlocal effects.

4. Conclusion

The results presented in this document provide important contributions to the ongoing investigation of the B flavour anomalies, which have emerged as potential hints of physics beyond the SM. The first analysis delivers a new measurement of the $R(D^+)$ and $R(D^{*+})$ ratios using muonic τ decays, a key test of LFU. The new measurements are consistent with the world averages and continue to exhibit a tension with the Standard Model predictions, now measured at a significance of 3.2σ. This reinforces the importance of future measurements.

The second analysis provides the first comprehensive study of both local and nonlocal contributions to the $B^0 \to K^{*0}\mu^+\mu^-$ decay. By disentangling local from nonlocal amplitudes, the analysis allows for a clearer view of potential NP contributions while accounting for significant nonlocal effects. The results, showing a 2.1σ deviation in the WC C_9, remain in broad agreement with previous measurements, suggesting that future studies with higher precision are necessary to resolve the full extent of any deviations from the Standard Model.

These new insights, particularly the ability to model nonlocal effects in rare B decays, represent a critical step toward fully understanding the B flavour anomalies. As more data is being collected in the Run 3 of data taking, the coming years will be decisive in determining whether these anomalies are a window into NP or a not yet understood effect of SM processes.

References

[1] LHCb collaboration, A. A. Alves Jr. *et al.*, *The LHCb detector at the LHC*, JINST **3** (2008) S08005.

[2] LHCb collaboration, R. Aaij *et al.*, *LHCb detector performance*, Int. J. Mod. Phys. **A30** (2015) 1530022, arXiv:1412.6352.

[3] Y. Amhis *et al.*, *Averages of b-hadron, c-hadron, and τ-lepton properties as of 2021*, Phys. Rev. **D107** (2023) 052008, arXiv:2206.07501, updated results and plots available at https://hflav.web.cern.ch.

[4] LHCb collaboration, R. Aaij *et al.*, *Differential branching fraction and angular analysis of the decay $B^0 \to K^{*0}\mu^+\mu^-$*, JHEP **08** (2013) 131, arXiv:1304.6325.

[5] LHCb collaboration, R. Aaij *et al.*, *Measurement of form-factor-independent observables in the decay $B^0 \to K^{*0}\mu^+\mu^-$*, Phys. Rev. Lett. **111** (2013) 191801, arXiv:1308.1707.

[6] LHCb collaboration, R. Aaij *et al.*, *Angular analysis of the $B^0 \to K^{*0}\mu^+\mu^-$ decay using $3\,fb^{-1}$ of integrated luminosity*, JHEP **02** (2016) 104, arXiv:1512.04442.

[7] LHCb collaboration, R. Aaij *et al.*, *Measurement of CP-averaged observables in the $B^0 \to K^{*0}\mu^+\mu^-$ decay*, Phys. Rev. Lett. **125** (2020) 011802, arXiv:2003.04831.

[8] LHCb collaboration, R. Aaij *et al.*, *Amplitude analysis of the $B^0 \to K^{*0}\mu^+\mu^-$ decay*, Phys. Rev. Lett. **132** (2024) 131801, arXiv:2312.09115.

[9] LHCb collaboration, R. Aaij *et al.*, *Measurement of the ratio of branching fractions $\mathcal{R}(D^*)$ and $\mathcal{R}(D^0)$* , Phys. Rev. Lett. **131** (2023) 111802, arXiv:2302.02886.

[10] LHCb collaboration, R. Aaij *et al.*, *Test of lepton flavour universality using $B^0 \to D^{*-}\tau^+\nu_\tau$ decays, with hadronic τ channels*, Phys. Rev. **D108** (2023) 012018, Erratum ibid. **D109** (2024) 119902, arXiv:2305.01463.

[11] LHCb collaboration, R. Aaij *et al.*, *Measurement of the branching fraction ratios $R(D^+)$ and $R(D^{*+})$ using muonic τ decays*, arXiv:2406.03387, Submitted to Phys. Review Letters.

[12] LHCb collaboration, R. Aaij *et al.*, *Comprehensive analysis of local and nonlocal amplitudes in the $B^0 \to K^{*0}\mu^+\mu^-$ decay*, JHEP **09** (2024) 026, arXiv:2405.17347.

[13] R. Aaij *et al.*, *Design and performance of the LHCb trigger and full real-time reconstruction in Run 2 of the LHC*, JINST **14** (2019) P04013, arXiv:1812.10790.

[14] M. Pivk and F. R. Le Diberder, *SPlot: A Statistical tool to unfold data distributions*, Nucl. Instrum. Meth. A **555** (2005) 356, arXiv:physics/0402083.

[15] S. de Boer, T. Kitahara, and I. Nišandžić, *Soft-Photon Corrections to $\overline{B} \to D\tau^-\overline{\nu}_\tau$ Relative to $\overline{B} \to D\mu^-\overline{\nu}_\mu$*, Phys. Rev. Lett. **120** (2018) 261804.

PoS(LHCP2024)079

[16] D. Bigi and P. Gambino, *Revisiting $B \to D\ell\nu$*, Phys. Rev. D **94** (2016) 094008.

[17] Fermilab Lattice, MILC, Fermilab Lattice, MILC, A. Bazavov *et al.*, *Semileptonic form factors for $B \to D^*\ell\nu$ at nonzero recoil from 2+1-flavor lattice QCD: Fermilab Lattice and MILC Collaborations*, Eur. Phys. J. C **82** (2022) 1141, arXiv:2105.14019, [Erratum: Eur.Phys.J.C 83, 21 (2023)].

[18] F. U. Bernlochner and Z. Ligeti, *Semileptonic $B_{(s)}$ decays to excited charmed mesons with e, μ, τ and searching for new physics with $R(D^{**})$*, Phys. Rev. D **95** (2017) 014022.

[19] F. U. Bernlochner *et al.*, *Das ist der HAMMER: Consistent new physics interpretations of semileptonic decays*, Eur. Phys. J. C **80** (2020) 883, arXiv:2002.00020.

[20] J. García Pardiñas *et al.*, *RooHammerModel: interfacing the HAMMER software tool with HistFactory and RooFit*, JINST **17** (2022) T04006, arXiv:2007.12605.

[21] W. Verkerke and D. Kirkby, *The roofit toolkit for data modeling*, 2003.

[22] Flavour Lattice Averaging Group, S. Aoki *et al.*, *FLAG Review 2019: Flavour Lattice Averaging Group (FLAG)*, Eur. Phys. J. C **80** (2020) 113, arXiv:1902.08191.

[23] S. Fajfer, J. F. Kamenik, and I. Nisandzic, *On the $B \to D^*\tau\bar{\nu}_\tau$ Sensitivity to New Physics*, Phys. Rev. D **85** (2012) 094025, arXiv:1203.2654.

[24] W. Altmannshofer *et al.*, *Symmetries and Asymmetries of $B \to K^*\mu^+\mu^-$ Decays in the Standard Model and Beyond*, JHEP **01** (2009) 019, arXiv:0811.1214.

[25] H. M. Asatrian, C. Greub, and J. Virto, *Exact NLO matching and analyticity in $b \to s\ell\ell$*, JHEP **04** (2020) 012, arXiv:1912.09099.